Energy Management for a Power-Split Plug-in Hybrid Electric Vehicle Based on Dynamic Programming and Neural Networks

Zheng Chen, *Member, IEEE*, Chunting Chris Mi, *Fellow, IEEE*, Jun Xu, *Student Member, IEEE*, Xianzhi Gong, and Chenwen You

***Abstract*—This paper focuses on building an efficient, online, and intelligent energy management controller to improve the fuel economy of a power-split plug-in hybrid electric vehicle (PHEV). Based on a detailed powertrain analysis, the battery current can be optimized to improve the fuel economy using dynamic programming (DP). Three types of drive cycles, i.e., highway, urban, and urban (congested), are classified, and six typical drive cycles are analyzed and simulated to study all the driving conditions. The online intelligent energy management controller is built, which consists of two neural network (NN) modules that are trained based on the optimized results obtained by DP methods, considering the trip length and duration. Based on whether the trip length and duration are known or unknown, the controller will choose the corresponding NN module to output the effective battery current commands to realize the energy management. Numerical simulation shows that the proposed controller can improve the fuel economy of the vehicle.**

***Index Terms*—Battery, dynamic programming (DP), neural network (NN), plug-in hybrid electric vehicle (PHEV), state of charge (SOC), trip length and duration.**

I. Introduction

HYBRID and plug-in electric vehicles (HEVs/PHEVs) have excellent fuel economy and environmental advantages [1]–[6]. HEVs and PHEVs are powered with two drivetrains, one or two electric motors, and an internal combustion engine (ICE). Managing the proper propulsion energy distribution between the two drivetrains [4], [5] becomes very essential and important. PHEVs, which are equipped with a larger energy storage system, represent the development trend of HEVs. In addition to working under a hybrid mode or a charge-sustaining (CS) mode, PHEVs can power the vehicle by using only the stored energy charged from the power grid; this is known as the charge-depleting (CD) mode [7]. This is the major difference between a PHEV and a HEV. It combines the merits of an HEV and an electric vehicle (EV). Thus, it is more important and more complicated to manage the energy distribution between the two drivetrains for a PHEV than for a HEV. An appropriate energy management strategy can improve the fuel economy, decrease the operation cost, and prolong the battery life without sacrificing the driving performance. The target of this paper is to propose an online and intelligent controller to improve the fuel economy of a PHEV.

Since a PHEV has the capability of all electric driving (AER), the simplest way to manage the energy distribution between its battery and ICE is to classify the vehicle running mode into two modes: CD and CS modes [7]. During the CD mode, the vehicle can be powered mostly by electric motors until the battery state of charge (SOC) [8] drops to a preset low threshold. After that, the vehicle changes into the CS mode, under which the vehicle works similar to a conventional HEV and maintains the SOC near the low threshold. This control algorithm is simple and easy to implement. However, it may not save fuel consumption in either CD or CS modes, as the motor and the ICE are only satisfying the propulsion demand without considering efficiency optimization and may not work in the high efficiency region.

Substantial research efforts have been carried out on the energy management of HEVs and PHEVs to improve fuel economy [4]–[6], [9]–[28] and to prolong battery life [14], [23] with or without the help of the GPS or a geographic information system (GIS) [29], [30]. The research methods can be classified into three categories: 1) analytic methods [4], [5], [9], [31]; 2) intelligent control algorithms such as fuzzy logic [13], [24], neural networks (NNs) [5], [11], [12], [22], model predictive control (MPC) [25], and genetic algorithms [10]; and 3) optimal theory methods such as minimum theory [16], [19] and DP methods [5], [11]–[13], [15], [20], [29], [32], which includes deterministic DP and stochastic DP. These various methods will be briefly discussed in the following.

1) Analytic Method: This type of method mainly focuses on powertrain analysis and is based on several running modes of PHEVs. In [9], intelligent CD control strategies and fuel optimization for a blended-mode PHEV were proposed with known electric system loss characteristics and other variables but without the detailed trip information. The proposed method cannot give an optimal solution for the energy management with simple analysis. In [31], a modern analytical approach was proposed for the power management of blended-mode PHEVs. The power management strategy was represented by a pair of power parameters that describe the power threshold

Manuscript received May 2, 2013; revised July 15, 2013; accepted October 11, 2013. Date of publication November 5, 2013; date of current version May 8, 2014. The review of this paper was coordinated by Mr. D. Diallo.

The authors are with the Department of Electrical and Computer Engineering, University of Michigan, Dearborn, MI 48128 USA (e-mail: botaoc@gmail.com; chrismi@umich.edu; xujun018@gmail.com; xianzhigong@gmail.com; youc@umich.edu).

Color versions of one or more of the figures in this paper are available online at http://ieeexplore.ieee.org.

Digital Object Identifier 10.1109/TVT.2013.2287102

for turning on the engine and the optimum battery power in engine-on operations. The target is a blended-mode PHEV, and the method is not universal for all PHEVs, including extended-range PHEVs.

2) Intelligent Method: In [5], [13], and [24]–[26], several typical intelligent methods, such as fuzzy logic, MPC, and NNs, are used to control the energy distribution in a HEV or PHEV. In [24], the battery working state (BWS) was used by a fuzzy logic energy management system of a PHEV to make the decision on the power-split ratio between the battery and the engine based on the BWS and vehicle power demand. The safety of the battery is of most importance in the paper. In [25], MPC-based energy management of a power-split HEV was introduced to obtain the power split between the ICE and the battery, whereas it did not consider the total trip length and full use of the battery.

3) Optimal Theory Method: Generally, optimal theory methods include the minimum theory and DP methods (including deterministic DP and stochastic DP). In [29] and [30], a trip-based optimal energy management method was proposed for PHEV based on a DP method. The proposed method requires the detailed trip information and needs too much calculation and computation time, which decreases the feasibility of application of the method. In [32], stochastic DP to optimize PHEV energy management was proposed with consideration of the fuel and electricity price. The method was based on a distribution of drive cycles and had the function of predicting road conditions. However, it still needs some considerable calculation, which increases the calculation burden of the vehicle controller when applied online. Moreover, it did not consider the whole trip length so that it may not use up all the available electric energy stored in the battery in a given trip. In [18], an intelligent multifeature statistical approach to automatically discriminate the driving condition of the HEV was proposed, and a support vector machine (SVM) method to intelligently and automatically discriminate the driving conditions was applied to classify the road pattern with high accuracy. It does not apply to a PHEV with a larger battery capacity. In [19], a model-based control approach for PHEV energy management to reduce the overall CO_2 emissions was introduced by applying the Pontryagin's minimum theory and by considering the electricity constitution in different countries and areas under known trip information as *a priori* knowledge. A machine learning framework that combines DP and quadratic programming was proposed in [11], [12], and [22]. Machine learning is used to know the roadway type and the traffic congestion level. They are only applied to HEVs with a small range of SOC variation.

Based on the earlier discussion, a conclusion can be made that an intelligent controller with fast calculation and excellent control performance is necessary for a PHEV. Given the detailed or basic trip information such as trip length and trip duration, the fuel economy can be improved. This is the main motivation of this paper. In this paper, the main target is to improve the fuel economy of a PHEV with known trip information such as trip length and trip duration. We selected a power-split PHEV as the research object. The PHEV has two motors/generators and is more complicated compared with a series or parallel PHEV. To build a fast, online, easy to implement, and effective energy management controller, we first applied an offline method, i.e., DP, to obtain the optimal energy distribution between the ICE and the battery by numerical calculations considering different road types. Then, based on the optimized results, an NN is introduced to train them to generate an online optimal energy controller with known trip length and trip duration.

The NN controller [11], [12], [22] includes a variety of formulas to store the optimal energy distribution information based on 1) vehicle speed; 2) acceleration/deceleration; 3) trip information, including trip length and duration; and 4) battery SOC. To build an effective NN controller, abundant vehicle simulation data based on the DP method are essential, which can include all driving conditions. In this paper, six standard drive cycles are used to simulate the vehicle operating condition, including 1) Urban Dynamometer Driving Schedule (UDDS); 2) SC03; 3) Highway Fuel Economy Driving Schedule (HWFET); 4) US06_HWY; 5) Manhattan (MANN); and 6) New York City Cycle (NYCC), which can represent the criteria of highway, urban, and congested urban driving conditions to test the light-duty vehicles in the U.S. Each drive cycle is simulated with multiple consecutive iterations to consider enough driving distances and duration.

Then, we applied the controller to drive scenarios with unknown trip information. It was shown that the proposed method can still save fuel consumption even without knowing the trip length or duration, although the benefits are significantly reduced.

II. Vehicle Model and Analysis

The objective in this paper is to optimize the fuel consumption of a power-split PHEV during a certain trip, which can be expressed as an optimization problem, i.e.,

$$\min F = \min \sum_{t=0}^{t=n} m_f(t,\, v) \tag{1}$$

where F is the total fuel consumption, n is the trip duration, and m_f is the fuel rate determined by engine speed w_e and engine torque T_e as follows:

$$m_f = f(T_e,\, w_e) \tag{2}$$

with f being a high nonlinear function.

To calculate m_f and optimize F, the vehicle powertrain should be analyzed in detail. The powertrain structure of the power-split PHEV analyzed in this paper is shown in Fig. 1. The vehicle includes a gasoline ICE, two electric motors, a lithium-ion battery pack, and a planetary gear set, which combines the engine, a motor, and the final driveline together with a particular gear ratio [5], [10]–[13].

In Fig. 1, the vehicle can be powered by the motor only, by the engine only, or by both. [5]. There exist several modes according to the power flow [10], [13], and it increases the analysis complexity of fuel rate. The vehicle driveline power P_o equals the sum of ring power P_r and motor-1 power P_{mot1}, i.e.,

$$P_o = T_o w_o = P_r + P_{\mathrm{mot1}} = T_r w_r + T_{\mathrm{mot1}} w_{\mathrm{mot1}} \tag{3}$$

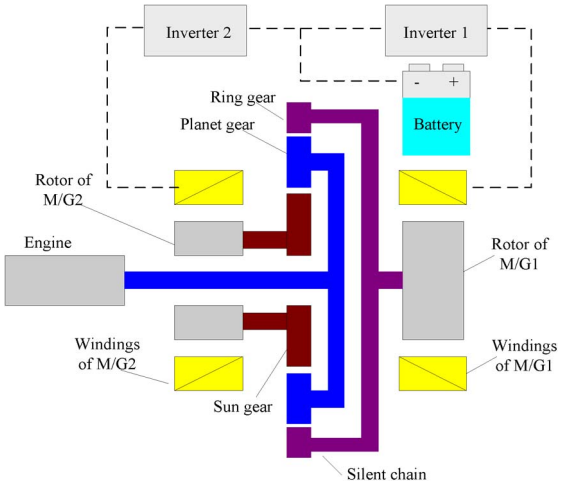

Fig. 1. Power-split vehicle powertrain.

where T_o, T_r, and T_{mot1} denote the torque of the driveline, the torque of the ring gear of the planetary gear set, and the torque of motor 1, respectively, and w_o, w_r, and w_{mot1} denote their speeds, respectively. Driveline torque T_o should satisfy

$$\begin{cases} T_o = (T_r + T_{\text{mot1}} r_{\text{mot1}}) \cdot r_{\text{final}} \\ w_{\text{mot1}} = w_o/(r_{\text{final}} r_{\text{mot1}}) \\ w_r = w_o/r_{\text{final}} \end{cases} \tag{4}$$

where r_{mot1} and r_{final} are the gear ratio between motor 1 and the driveline and the driveline and vehicle wheels, respectively. The planetary gear set consists of a sun gear, a ring gear, and a carrier, which connects motor 2, the driveline, and the engine, respectively. Neglecting the friction and inertia losses, there are two basic equations for the speed and torque of the planetary gear set, i.e.,

$$\begin{cases} (1+\rho) \cdot w_e = \rho \cdot w_{\text{mot2}} + w_r \\ T_e = (1 + 1/\rho) \cdot T_{\text{mot2}} = (1+\rho) \cdot T_r \end{cases} \tag{5}$$

where ρ is the ratio of the sun gear and the ring gear; w_e and w_{mot2} represent the speed of the engine and motor 2, respectively; and T_e and T_{mot2} are their torque, respectively. Based on (3)–(5), we can calculate T_e further as follows:

$$T_e = \frac{1}{1+\rho} \cdot \frac{T_o - P_b \cdot \eta_{\text{mot1}}}{r_{\text{final}} w_o} + \frac{1}{(1+\rho)^2} \cdot \frac{((1+\rho) \cdot w_e - r_{\text{final}} w_o)}{r_{\text{final}} w_o} \cdot \frac{\eta_{\text{mot1}}}{\eta_{\text{mot2}}} \cdot T_e \tag{6}$$

where η_{mot1} and η_{mot2} are the efficiency of motors 1 and 2, respectively, and P_b and P_{mot2} are the power of the battery and motor 2, respectively. Solving (6), we can get

$$\begin{aligned} T_e &= \frac{\frac{1}{1+\rho} \cdot \frac{T_o - P_b \cdot \eta_{\text{mot1}}}{r_{\text{final}} w_o}}{1 - \frac{1}{(1+\rho)^2} \cdot \frac{((1+\rho) \cdot w_e - r_{\text{final}} w_o)}{r_{\text{final}} w_o} \cdot \frac{\eta_{\text{mot1}}}{\eta_{\text{mot2}}}} \\ &= g(T_o, P_b, w_o, w_e). \end{aligned} \tag{7}$$

From (7), T_e can be determined by T_o, P_b, w_o, and w_e. As T_o and w_o are determined to satisfy the vehicle torque demand and cannot be influenced by control algorithms, T_e can be controlled by different w_e and P_b. P_b can be approximately calculated by battery current I, battery open-circuit voltage V_{ocv}, and battery internal resistance R [10]–[12] as follows:

$$P_b = V_{\text{ocv}} I + I^2 R. \tag{8}$$

Hence, (2) can be changed into

$$m_f = f(T_e, w_e) = f_{\text{new}}(I, w_e). \tag{9}$$

Now, we can see that w_e and I can influence the fuel rate and can be therefore optimized to minimize the fuel consumption for a given trip. The calculation process includes some nonlinear efficiency coefficients, such as η_{mot1}, η_{mot2}, and fuel rate function f, which makes it not realistic to solve m_f based on (3)–(9). Therefore, Pontryagin's minimum principle [16], [19] is not appropriate for the optimization of fuel consumption. It needs to build a deterministic relationship between the input and the output, construct a Hamiltonian function, consider a proper boundary for each variable, and solve the partial differential function. DP [11], [12], [21], [33] does not need to get a detailed numerical solution, can easily apply the constraint of each variable, and can be easily applied in the discrete system. Based on the given discussion, we use DP to solve the energy management problem.

III. Dynamic Programming

DP is a numerical technique that can be applied to any problem that requires decisions to be made in stages with the objective of finding a minimal penalty decision pathway [5], [11]–[13], [20], [21]. DP combines knowledge of the immediate penalty of the decision at hand with knowledge of future penalties that arise as a result of the immediate decision. DP is commonly used for global optimization of the energy management of HEVs [11]–[13], [20]. Generally, it needs to define the constraints of each variable used to realize the DP algorithm and the grid size, which can determine the calculation precision and time consumption.

As discussed in Section II, battery current I and engine speed w_e influence the fuel rate and can be regarded as the controlled variables to realize the DP algorithm. However, it induces two degrees of freedom of optimization, which brings too much computation and high calculation cost [11], [12]. To simplify the calculation without influencing the precision, a method is proposed to convert the two-degree-of-freedom problem into a one-degree-of-freedom problem. For each operating point, we can find out the optimal operating efficiency point according to different engine power. In this way, at each engine operating power, we can determine the optimal engine speed w_e accordingly. This means that the engine can only work in the highest efficiency region at different power levels, and the fuel rate can only be determined by engine torque T_e. Fig. 2 shows the relationship between engine power P_e and speed w_e with an increment of 1 kW for the succeeding step. Based on this relationship, we can easily find the relationship between w_e and T_e, i.e.,

$$w_e = g_1(T_e). \tag{10}$$

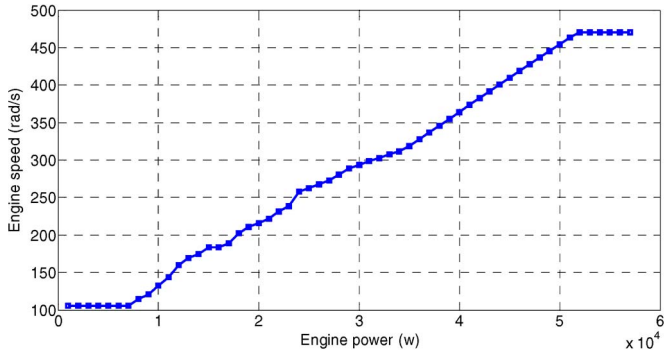

Fig. 2. Optimal speed profile at different engine power outputs.

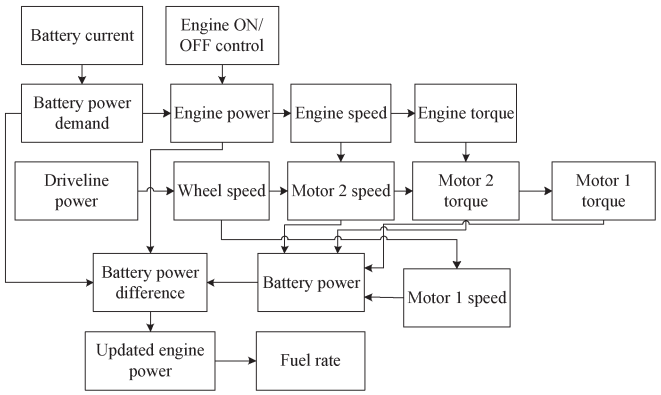

Fig. 3. Calculation process.

Now, based on (7)–(10), we can solve the fuel rate based on battery current I only. With different I commands, the motor power can be determined accordingly, and the engine power and engine fuel rate can be calculated. As presented in (6)–(9), we need to know the relationship between the motor efficiency and the fuel rate when calculating the fuel rate, which cannot be obtained directly. Here, we use a distributed computing method to get the fuel rate from the battery current [11], [12]. Equations (11)–(21) detail the calculation, and Fig. 3 shows the calculation process. First, motor 1 speed can be determined by the vehicle speed

$$w_{\text{mot1}} = w_{\text{ring}} = \frac{v_s}{\text{wheel\_}r} \times r_{\text{final}} \tag{11}$$

where $\text{wheel\_}r$ is the wheel radius, and v_s is the vehicle speed.

Based on different I, we can calculate the temporary engine power as follows:

$$P_e^* = P_{\text{drive}} + P_b + P_L = V_{\text{ocv}} I + I^2 R + P_o + P_L \tag{12}$$

where P_L is the accessory power of the vehicle, and P_e^* is the temporary engine power. According to the relationship in (10), the speed and torque of the engine and motor 2 can be calculated as follows:

$$w_{\text{mot2}} = w_e \left(1 + \frac{1}{\rho}\right) - w_{\text{mot1}} \frac{1}{\rho} \tag{13}$$

$$T_{\text{mot2}} = \frac{\rho}{\rho + 1} T_e^* \tag{14}$$

where T_e^* is the temporary engine torque. Based on the engine torque, we can calculate the ring torque and motor 1 torque accordingly

$$T_{\text{ring}} = \frac{1}{1+\rho} T_e^* \tag{15}$$

$$\begin{aligned} P_o &= P_{\text{mot1}} + P_{\text{ring}} = T_{\text{ring}} w_{\text{ring}} + T_{\text{mot1}} \omega_{\text{mot1}} \\ &= (T_{\text{ring}} + T_{\text{mot1}}) \omega_{\text{mot1}} \end{aligned} \tag{16}$$

$$T_{\text{mot1}} = \frac{P_o}{w_{\text{mot1}}} - T_{\text{ring}}. \tag{17}$$

We have already known the motor speed and torque; thus, the motor efficiency and losses can be determined as follows:

$$\begin{cases} P_{\text{mot1\_loss}} = (1 - \eta_{\text{mot1}}) T_{\text{mot1}} w_{\text{mot1}} \\ P_{\text{mot2\_loss}} = (1 - \eta_{\text{mot2}}) T_{\text{mot2}} w_{\text{mot2}} \end{cases} \tag{18}$$

where η_{mot1} and η_{mot2} are the efficiency of motors 1 and 2. The updated engine power and torque can be obtained by the sum of temporary engine power and motor losses as follows:

$$\begin{aligned} P_e &= P_e^* + P_{\text{mot1\_loss}} + P_{\text{mot2\_loss}} \\ &= P_o + P_b + P_L + P_{\text{mot1\_loss}} + P_{\text{mot2\_loss}} \\ &= V_{\text{ocv}} I + I^2 R + P_L + P_o + P_{\text{mot1\_loss}} + P_{\text{mot2\_loss}}. \end{aligned} \tag{19}$$

Based on the new engine power P_e, engine torque T_e and engine speed w_e can be determined by (10); finally, the updated engine fuel rate can be calculated. It is worth pointing out that the motor speed and torque may vary with the new engine speed and torque; we assume their efficiency are kept unchanged during the calculation, i.e.,

$$\tau_{\text{eng}} = P_{\text{eng}} / w_{\text{eng}} \tag{20}$$

$$f(w_{\text{eng}}, \tau_{\text{eng}}) = f_{\text{new2}}(I). \tag{21}$$

To realize DP, some constraints [11], [12], [21] should be considered, such as engine maximum power, engine maximum and minimum speed, battery maximum charge and discharge current, and motor maximum and minimum power as follows:

$$\begin{cases} 0 \le P_e \le P_{\max},\ w_{\min} \le w_e \le w_{\max} \\ P_{\text{mot1\_min}} \le P_{\text{mot1}} \le P_{\text{mot1\_max}} \\ P_{\text{mot2\_min}} \le P_{\text{mot2}} \le P_{\text{mot2\_max}} \\ P_{b\_\min} \le P_b \le P_{b\_\max} \\ C_{b\_\min} \le C_b \le C_{b\_\max} \end{cases} \tag{22}$$

where the subscript "min" and "max" denote the minimum and maximum values of each variable, respectively, and C_b is the battery capacity in ampere-seconds. To realize DP, a cost-to-go matrix should be built, in which some variables, such as time interval Δt, total length t_{total}, and grid size ΔC_b should be determined.

Due to the bounds of energy, certain grid levels between $C_{b\_\min}$ and $C_{b\_\max}$ needs to be determined [5], [20]. This area is mapped onto a fixed grid with determined distance ΔC_b, so that $m+1$ capacity levels are considered

$$m = \left\lfloor \frac{C_{b\_\max} - C_{b\_\min}}{\Delta C_b} \right\rfloor. \tag{23}$$

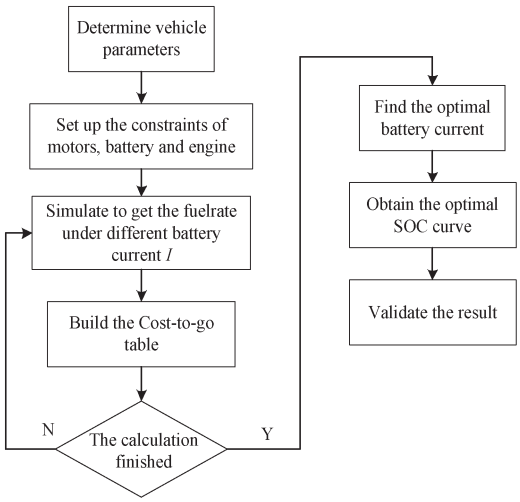

Fig. 4. Procedure of the realizing DP method.

TABLE I
VEHICLE PARAMETERS

Vehicle type	Plug-in split HEV
Vehicle mass	1641.3kg
Engine power	57kW
Motor power	25kW, peak power 50kW
Generator power	15kW, peak power 30kW
Planetary gear set	Sun gear 30 Ring gear 78
Battery	Lithium-ion battery Rated capacity 20Ah Rated voltage 356V

The optimal values are calculated afterward, by starting at $C_b(n)$ (n is the duration of drive cycle) and then following the path of minimal cost. Given the sequence of I, the requested set points for the motor and the generator are found. All calculations required for DP can be done in a reasonable amount of time due to the simple dynamics and all the restrictions of I, C_b, w_e, P_{mot1}, P_{mot2}, and P_e. However, the computation rapidly increases with the driving cycle length and the grid density [20], particularly when we apply several consecutive drive cycles. Considering the computation complexity and precision, we set $\Delta t = 1s$.

The steps to realize DP are shown in Fig. 4. First, the constraints of the motors, the battery, and the engine should be properly considered, and the engine fuel rate can be calculated according to (11)–(21) with different battery currents. At the same time, the cost-to-go matrix can be built. After getting the cost-to-go matrix, the optimal SOC curves and the optimal battery current with different beginning SOCs can be obtained. The last step is to validate the result as we missed some issues, such as inertia of the motors and the engine, and simplified some variables during the calculations. Table I lists the vehicle parameters.

IV. DYNAMIC PROGRAMMING RESULT: ANALYSIS AND APPLICATION

We need to validate the DP results through simulation and analysis. Due to the high nonlinearity of the vehicle system, it is difficult to get the optimal result by approximating it to a linear or quadratic system. If we can simulate the vehicle with a constant-speed profile, we can simplify the problem and analyze the result using the linear programming (LP) method to prove the correctness of the DP result. Here, the whole validation is divided into two parts: 1) constant-speed simulation; and 2) drive cycle simulation. Before analyzing the fuel consumption, the default control algorithm, i.e., the CD and CS strategies, is applied to simulate and obtain the vehicle performance as a reference [7]. Considering the calculation cost, the current grid is set to 14.4 A. According to the constraints of the battery, the current grid matrix can be built as follows:

$$I = [-100.8, -86.4, -72.0, -57.6, -43.2, -28.8, -14.4, 0, 14.4, 28.8, 43.2, 57.6, 72.0, 86.4, 100.8]. \quad (24)$$

At each step, the optimal battery current command can be selected from (24) to minimize the fuel consumption.

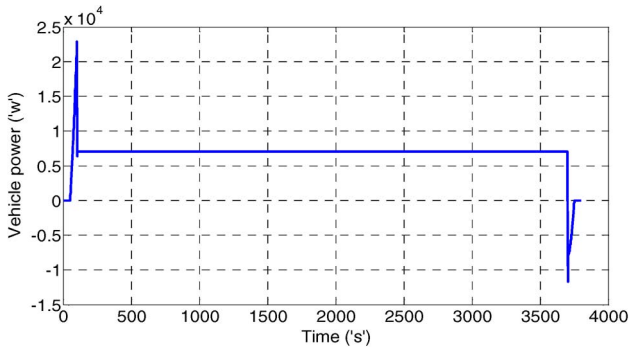

Fig. 5. Power demand of 50-mi/h constant-speed drive cycle.

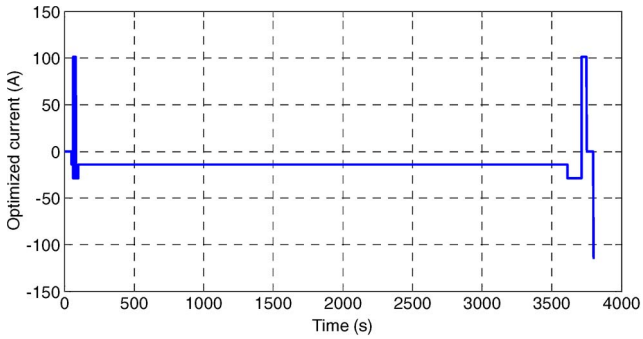

Fig. 6. Battery current obtained by DP method.

A. Constant Speed Simulation

We built the drive cycles with a constant-speed driving time at 3600 s and the vehicle is at rest for 50 s at the beginning and at the ending. The acceleration is 1 mi/h/s in the beginning after rest time, and the deceleration is -1 mi/h/s after the constant-speed driving. Therefore, the total time of 50-mi/h drive cycle equals 3800 s. The vehicle driveline power demand during the whole drive cycle is shown in Fig. 5. The maximum power is 22.84 kW, and the constant power is 7.04 kW when the vehicle speed stabilizes at 50 mi/h.

The optimized battery current based on the DP method is shown in Fig. 6. From 100 to 3700 s, the battery is discharged

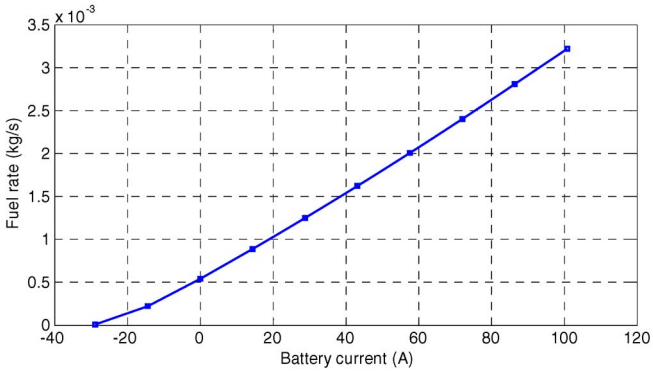

Fig. 7. Fuel rate for the 50-mi/h constant-speed drive cycle.

with a current of 14.4 A for 3511 s, followed by a current of 28.8 A for 89 s. During this period, as the vehicle power demand is unchanged, it is easy to apply the analytical method to validate the DP result. The driveline power is 7.04 kW, and if the vehicle can be driven by the battery only, the current is about 30 A. Therefore, the available battery current range becomes

$$I = [-28.8,\ -14.4,\ 0,\ 14.4,\ 28.8,\ 43.2,\ 57.6,\ 72.0,\ 86.4,\ 100.8]. \quad (25)$$

Fig. 7 shows the fuel rates with different battery currents according to (11)–(21), and they range from 0.00001 to 0.00322 kg/s. We implemented the LP method [34] to validate the DP result. From (25), as there are only ten selections, we can calculate the following equations to get the optimal value:

$$F = \min(a_1 \cdot x_1 + a_2 \cdot x_2 + a_3 \cdot x_3 + \cdots + a_9 \cdot x_9 + a_{10} \cdot x_{10})$$

$$\begin{cases} \sum_{i=1}^{10} x_i = 3600 \\ -28.8 \cdot x_1 - 14.4 \cdot x_2 + 0 \cdot x_3 + 14.4 \\ \quad \cdot x_4 + \cdots + 100.8 \cdot x_{10} = \Delta soc \cdot C_b \\ x_i \geq 0, (i = 1, 2, \ldots, 10) \\ x_i \in \text{Integers} \end{cases} \quad (26)$$

where $x_i (i = 1, 2, \ldots, 10)$ denote the duration time for each current state of (25), are integers, and should not be less than zero. The sum of $x_i (i = 1, 2, \ldots, 10)$ should equal 3600. a_1, $\ldots, a_{10}$ are fuel rates shown in Fig. 7. C_b equals 72 000. Δsoc is the SOC range from 100 to 3700 s and equals 0.7378. Using the LP method, the solution can be easily obtained as follows:

$$\begin{cases} x_1 = 89 \\ x_2 = 3511 \\ x_3 = x_4 = x_5 = x_6 = x_7 = x_8 = x_9 = x_{10} = 0. \end{cases} \quad (27)$$

The result shown in (27) is identical with the result shown in Fig. 6. Therefore, the DP result turned out to be correct by the LP method. However, the LP method can only be used to analyze the constant vehicle power optimization and cannot be used for the energy management for the PHEV as the vehicle speed and power could always change.

TABLE II
CONSTANT-SPEED DRIVE-CYCLE RESULT COMPARISON

Vehicle speed (mph)	Trip length (mile)	Duration (s)	Ending SOC (%)		Fuel consumption (kg)		Fuel savings (%)
			Default	DP	Default	DP (SOC corrected)	
30	30.26	3760	56.44	56.53	-	0.0016	-
40	40.46	3780	31.94	29.76	0.118	0.113	4.24
50	50.71	3800	32.21	30.68	1.083	1.045	3.51
60	61.02	3820	32.44	30.92	2.164	2.139	1.16
70	71.38	3840	32.63	31.08	3.503	3.546	-1.23

It is necessary to use the SOC correction method to update the fuel consumption to compare the fuel saving at the same SOC. Linear regression can be used to ensure that the initial and final SOCs are the same. Linear fitting was adopted to obtain fuel consumption and corrected with SOC [9], [31]. Table II shows the results with different constant-speed drive cycles. We can see that, when the vehicle speed is constant at 40, 50, and 60 mi/h, the DP method can save 4.24%, 3.51%, and 1.16% of the fuel, respectively. In this way, it shows the effectiveness of the DP method. However, for constant speed of 30 and 70 mi/h, DP does not show fuel savings. For the 30-mi/h drive cycle, when the default algorithm is applied, the engine is always off, and the vehicle is powered by the battery only. However, when the DP method is applied, the engine starts during the acceleration period, which induces some fuel consumption. For the 70-mi/h drive cycle, when the default algorithm is applied, the engine and motors work in the high efficiency region, and their speeds are unchanged. However, when the DP method is applied, the variation of battery current commands can make the motors and engine accelerate or decelerate, which costs more fuel consumption. Hence, the proposed algorithm is more suitable for drive speed between 30 and 70 mi/h. In real-world driving, constant-speed driving rarely happens. Therefore, we predict that the proposed DP algorithm can help save fuel as long as the vehicle is driven mostly between 30 and 70 mi/h. This is also validated through real-world driving cycle simulations in the following.

B. Drive Cycle Simulation

Several typical drive cycles are introduced to validate the DP algorithm. UDDS, which is also called "LA4" or "the city test," and SC03 drive cycles represent city driving conditions. HWFET and US06_HWY drive cycles represent highway driving conditions. NYCC and MANN drive cycles represent the congested-city drive cycles [18]. Fig. 8 shows two of these six drive cycles. Table III presents the total length, duration, the maximum speed, and the average speed for each drive cycle. It needs to be mentioned that, as the NYCC and MANN cycle lengths are very short, we repeated them three times as new drive cycles.

To compare the results, the default algorithm, i.e., the CD and CS method, was applied in the simulation to get the fuel consumption under different drive cycles. During CD mode, the vehicle is powered by the battery only. When the SOC drops near 30%, the vehicle is powered by the battery and the engine

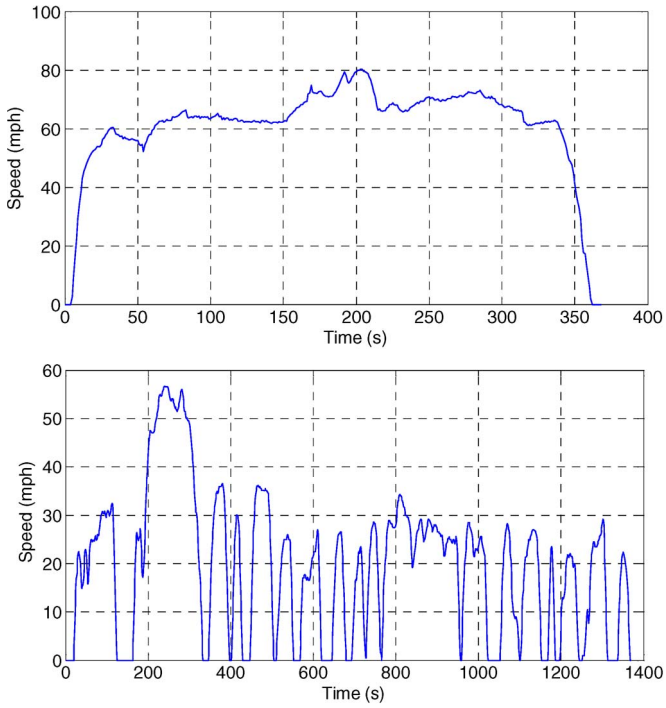

Fig. 8. Highway and urban drive cycles.

TABLE III
DRIVE-CYCLE COMPARISON

Type	Drive cycle	Length (miles)	Duration (s)	Maximum speed (mph)	Average speed (mph)
Freeway	HWFET	10.26	765	59.9	48.30
	US06_HWY	6.24	368	80.3	61.00
Urban	UDDS	7.45	1369	56.7	19.59
	SC03	3.60	596	54.8	21.60
Urban congested	3 NYCC	3.54	1794	27.7	7.10
	3 MANN	6.21	3267	25.4	6.80

together, which makes the battery SOC maintain at the low-preset threshold. The battery power is detailed in (28), shown at the bottom of the page, where $\min(\cdot)$ and $\max(\cdot)$ denotes the minimum and maximum values of the two values given in the parenthesis, respectively, and $P_{e\_\max}$ is the maximum engine power. The engine's output should satisfy the demand of the driveline power and battery power.

The initial battery SOC is supposed to be 100%. Figs. 9 and 10 show the battery SOC variation and engine fuel rates under the UDDS driving cycle test. Before 5300 s, the engine is off, and the vehicle is powered by the battery and motors. When the battery SOC decreases to 30%, the engine starts, the vehicle works in CS mode, and the battery SOC maintains near 30%.

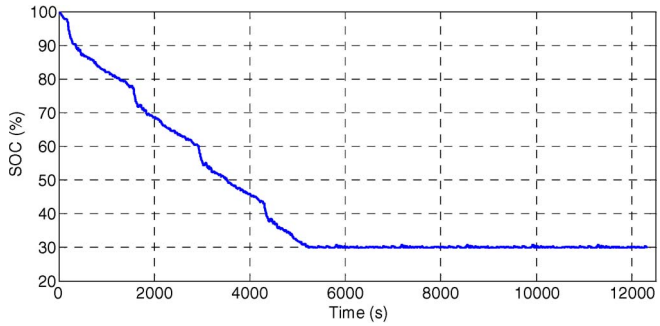

Fig. 9. Battery SOC variation.

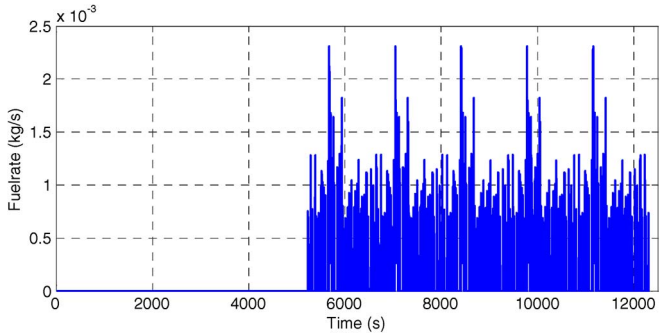

Fig. 10. Engine fuel rate.

The fuel consumption levels under UDDS and HWFET drive cycles are listed in Table IV. Fig. 11 shows the optimal SOC curves with different beginning SOC values under nine US06_HWY drive cycles and five UDDS drive cycles. In Fig. 11, the beginning SOC is from 100% to 30% with 10% decrement for the succeeding step. Fig. 12 compares the total fuel consumption with different drive cycles, in which the fuel savings are 0.30%, 4.12%, 3.94%, 3.82%, 3.86%, and 3.77% with four to nine US06_HWY drive cycles, ranging from 12.63% to 2.85% with four to nine HWFET drive cycles, and from 14.91% to 4.92% with five to nine UDDS drive cycles, respectively.

Fig. 13 shows a comparison of the difference of the battery current in eight consecutive UDDS drive cycles when the different algorithms are applied. We can see that, with the default algorithm, the battery is discharged more quickly than with the DP method. Fig. 14 compares the engine efficiency levels based on different algorithms. It can be seen that, when the DP method is applied, the engine average efficiency is higher than that when the default algorithm is applied. To some extent, the comparisons can explain why the DP method can save fuel consumption.

$$P_b = \begin{cases} P_o & \text{SOC} > 36\% \\ \min(31647, P_o) & 33\% \le \text{SOC} < 36\% \\ \min\left(31647 \cdot (\text{SOC} - 0.3)/0.03, P_o\right) & 30\% \le \text{SOC} < 33\% \\ \max\left(-30717 \cdot (\text{SOC} - 0.3)/0.03, P_o\right) & P_o < 0, 27\% \le \text{SOC} < 30\% \\ \max\left(-30717 \cdot (\text{SOC} - 0.3)/0.03, P_o - P_{e\_\max}\right) & P_o > 0, 27\% \le \text{SOC} < 30\% \\ \max(-30717, P_o) & P_o < 0, \text{SOC} < 27\% \\ \max(-30717, P_o - P_{e\_\max}) & P_o > 0, \text{SOC} < 27\% \end{cases} \quad (28)$$

TABLE IV
FUEL CONSUMPTION BASED ON CD/CS STRATEGY

Cycle Name	UDDS					HWFET				
No. of cycles	5	6	7	8	9	4	5	6	7	8	9
Distance (miles)	37.22	44.66	52.10	59.54	66.98	41.02	51.28	61.53	71.79	82.04	92.30
Fuel consumption (kg)	0.314	0.668	0.926	1.183	1.450	0.756	1.200	1.645	2.089	2.542	3.004

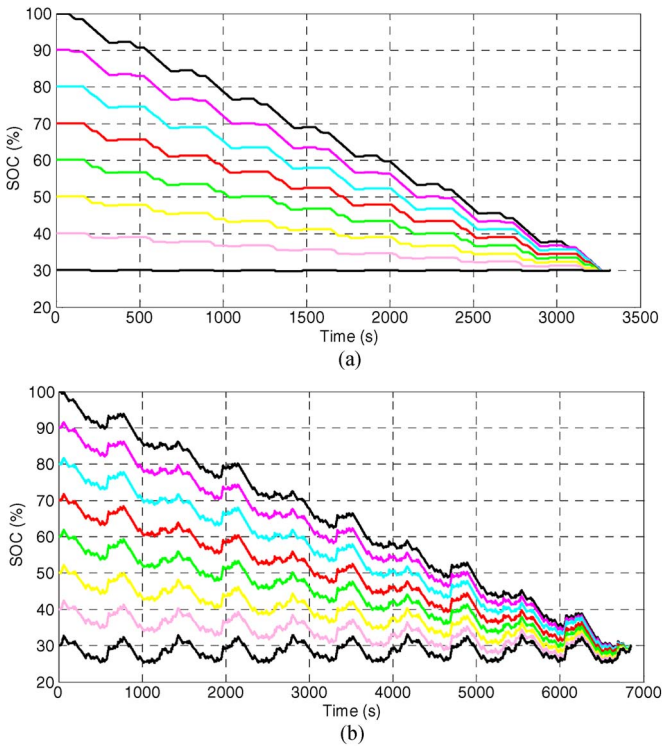

Fig. 11. Optimal SOC curve. (a) Optimal SOC curve based on nine consecutive US06_HWY drive cycles. (b) Optimal SOC curve based on five consecutive UDDS drive cycles.

V. NEURAL NETWORK TRAINING

As shown earlier, the DP result can improve fuel economy on conditions that the detailed trip information is known in advance. Moreover, it also needs a large amount of computation. These limit the real-time application of the DP algorithm. However, the optimal battery SOC and battery current values obtained by the DP method can be regarded as a benchmark for further study. It is necessary to construct an online and effective controller based on the DP result to realize real-time control. It is difficult to get a deterministic equation or relationship as the energy management strategy is influenced by many factors, such as acceleration, speed, battery SOC, trip length, trip duration, etc. An NN can effectively learn the nonlinear relationship based on the optimized results and can generate an online controller to manage the energy distribution. Here, we apply an NN to build an intelligent online controller to control the battery current and, consequently, the engine torque and speed to improve the fuel economy. The controller, as shown in Fig. 15, consists of two NN modules, i.e., N1 and N2, as shown in Figs. 16 and 17, respectively. The major difference between N1 and N2 is that N1 needs the trip information, i.e., trip duration and trip length. The principle of the controller is detailed in the following steps.

1) The beginning SOC is more than 30%, and the trip length and trip duration are known or estimated before the trip starts. In this case, if the trip length is less than AER according to calculation based on the beginning SOC, the controller will adopt the CD strategy and use the energy stored in the battery. Otherwise, the controller will select N1 as the controller to output the battery current commands to control the engine accordingly.
2) The beginning SOC is more than 30%, and the trip information is unknown. In this case, the controller will use the electric energy until the SOC drops to 30%. Then, the controller will select N2 to output the battery current command.
3) If the beginning SOC is not more than 30%, the controller will select N2 to output the battery current directly.

The function of N1 is to output the battery current command based on the basic trip information. It needs the total trip length and trip duration in advance. Therefore, it contains at least four variables: trip length, trip duration, current drive length, and current drive time. In [11], [12], and [22], the vehicle speed, driveline power, battery SOC, and the driving trend are utilized to train the NN to output the optimal battery power for a conventional HEV. Moreover, the authors also employed another NN module to predict the road pattern based on 11 variables, which brings too much complexity. In [18], four variables, i.e., average speed, idle rate, maximum acceleration, and minimum acceleration over a certain time interval, are applied to classify the driving patterns, of which the idle rate is the ratio of vehicle idle time during a certain time range. We combine them and select vehicle speed, driveline power, battery SOC, average speed, idle rate, maximum acceleration, and minimum acceleration to train the controller to ensure the system precision. Therefore, N1 in total consists of the aforementioned 11 variables. Compared with [11], [12], and [22], the energy management strategy proposed in this paper is easier to apply for energy management of a PHEV. During simulation, the time interval for calculating the average speed, the maximum acceleration, the minimum acceleration, and the idle rate is 50, 50, 50, and 100 s, respectively. The output of N1 is the battery current command. The beginning SOC to train the N1 is from 100% to 40% with 10% decrement for the succeeding step. We select the total drive cycle data, including UDDS, HWFET, US06_HWY, SC03, NYCC, and MANN cycles trained to generate N1.

Compared with N1, N2 does not consider the trip information and only has seven inputs, which are vehicle speed, vehicle driveline power, battery SOC, average speed, idle rate, maximum acceleration, and minimum acceleration. The beginning

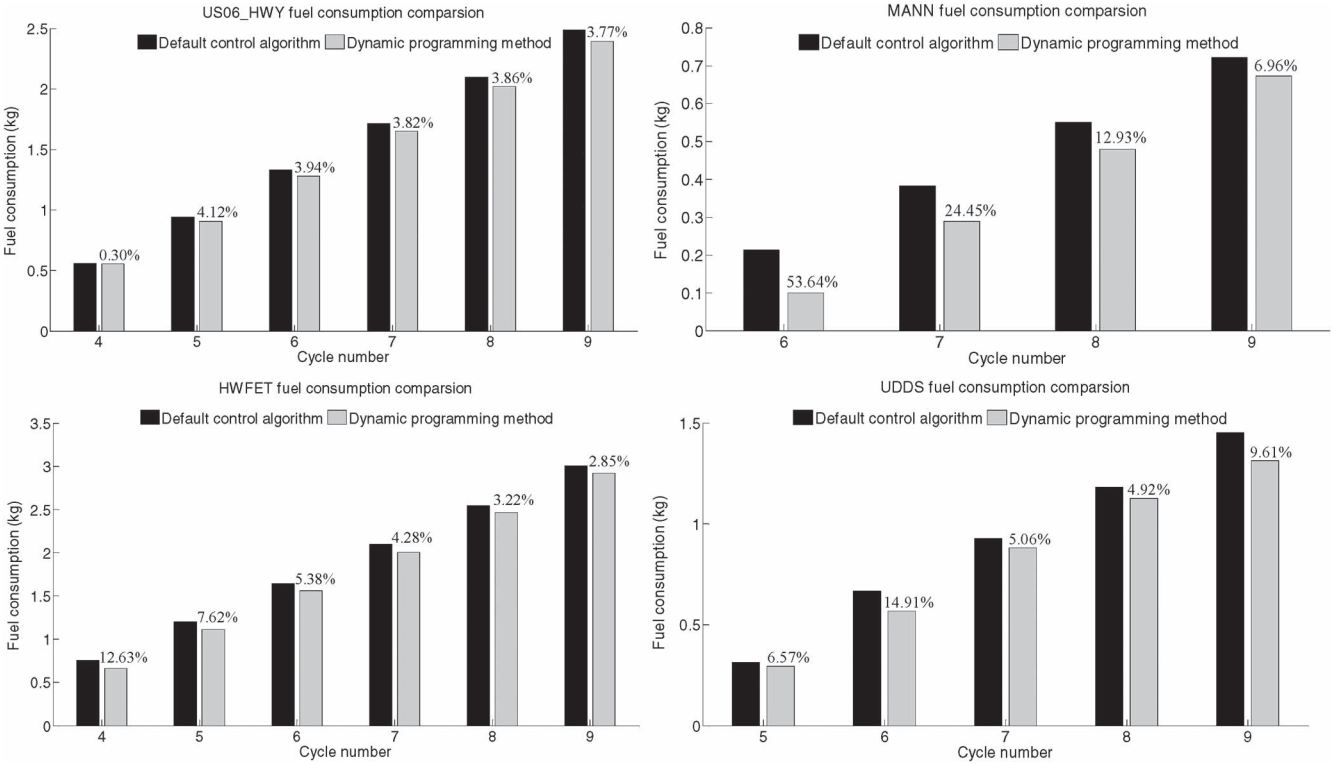

Fig. 12. Fuel consumption comparison under US06_HWY, MANN, HWFET, and UDDS drive cycles.

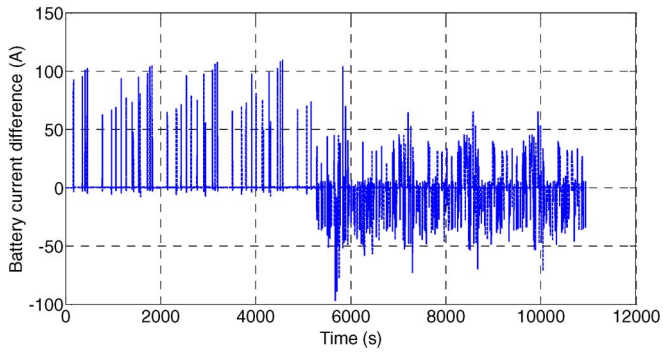

Fig. 13. Current difference.

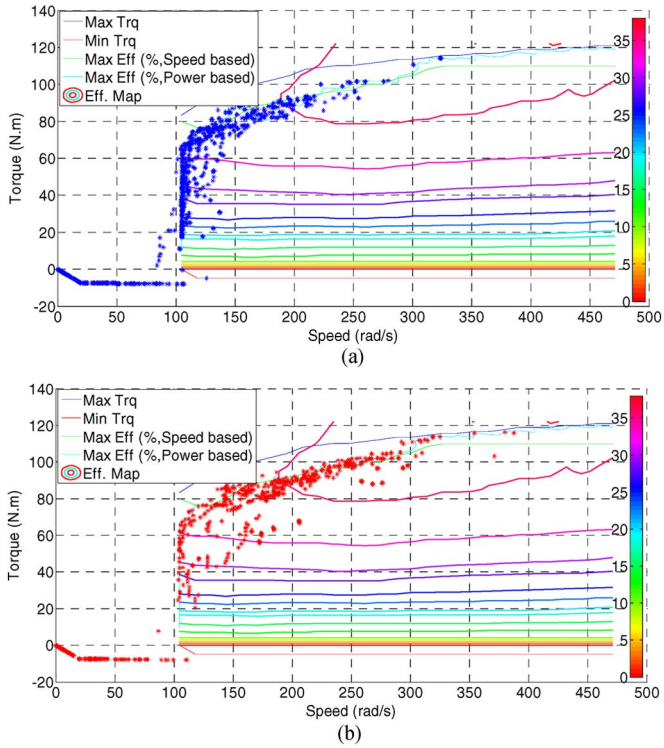

Fig. 14. Engine operating efficiency map. (a) Based on the CS and CD algorithm. (b) Based on the DP method.

SOC of N2 is 30%. The output is the same as N1. The NN training performance is measured by MSEs E_{MSE}, as shown in the following [11], [12]:

$$E_{\mathrm{MSE}} = \frac{1}{N}\sum_{i=1}^{N}(y(i) - y_t(i))^2 \tag{29}$$

where $y(i)$ is the NN output, and $y_t(i)$ is the target data. In the training process of N2, the target of E_{MSE} is 0.001, and N equals 7075. Fig. 18 compares the trained data and actual output, and shows their differences for N2. We can see the controller can output the battery current effectively, and the maximum error is less than 10 A.

VI. Result Validation

According to the description of the controller in Section V, when the trip length and trip duration are known in advance and the trip length is more than the AER calculated by the battery initial SOC, the controller will use N1 to output the battery current commands to manage the power distribution between the ICE and the battery. Usually, the trip length and trip duration

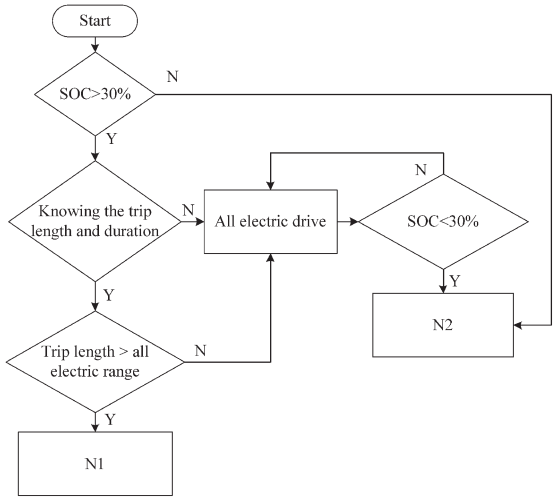

Fig. 15. Vehicle controller.

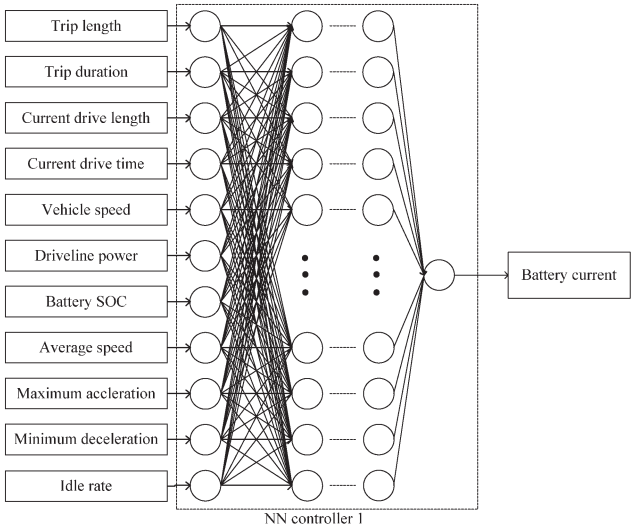

Fig. 16. NN controller N1.

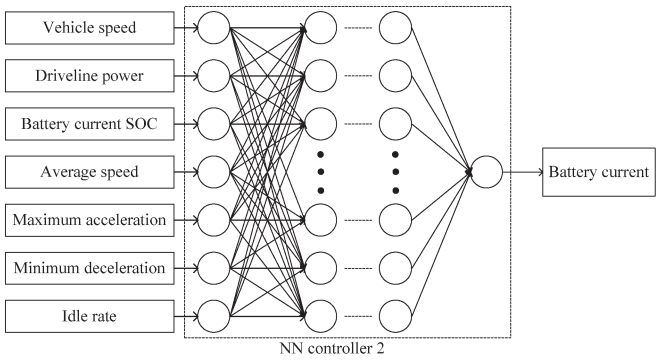

Fig. 17. NN controller N2.

can be determined with the help of GPS/GIS or be estimated by experience. If the controller cannot obtain them before the trip starts, it will use the battery to power the vehicle first until the battery SOC drops to a preset low threshold (30%) and then use N2 to control the battery power.

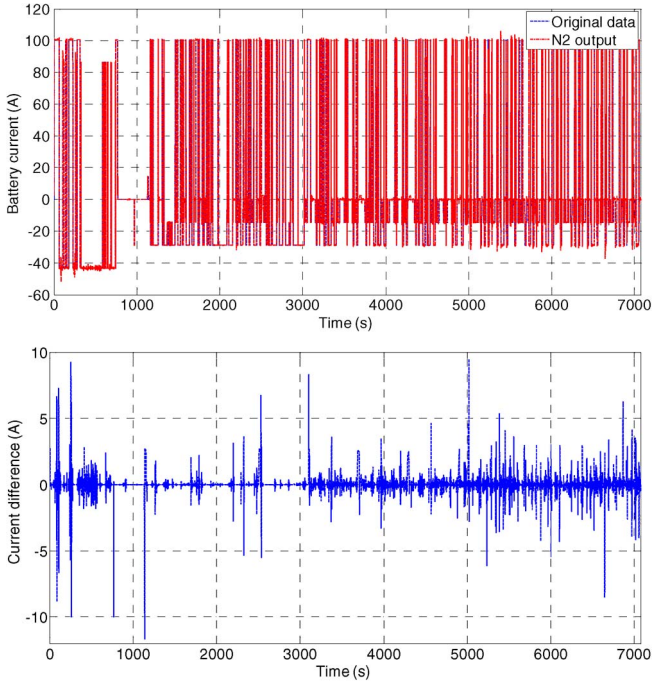

Fig. 18. Training result of N2.

A. Simulation With Knowing the Trip Length and Duration Precisely

Suppose the controller knows the trip length and duration precisely by GPS beforehand, we applied LA092 and REP05 drive cycles to validate the controller's performance.

The LA92 drive cycle's maximum speed is 67.30 mi/h, and its average speed is 24.61 mi/h; it can represent the urban driving condition. The REP05 drive cycle can be mainly split into two parts, i.e., highway and urban driving, and its maximum speed is 80.20 mi/h. These two drive cycles can include highway and urban driving conditions. Here, we select LA92 cycle repeating four and six times, and REP05 cycle repeating two and three times to make sure the trip lengths are more than the maximum AER. The beginning SOC is 100%; the total driving distance is 39.24, 58.86, 40.08, and 60.12 mi; and the time duration are 5740, 8610, 2800, and 4200 s, respectively. As shown in Table V, using the proposed controller, the fuel consumption can be reduced by 3.96%, 3.88%, 2.20%, and 2.79% with SOC correction included.

Fig. 19 compares the SOC variation when the two control algorithms are applied for four LA92 drive cycles, where we can see the SOC drops slower when the proposed controller is applied than that when the CD and CS algorithm is applied. Fig. 20 compares the engine operating efficiency levels. We can see that the engine works more efficiently when the proposed controller is applied. This way, it can prove that the controller can improve the fuel economy.

B. Simulation With Estimation of the Trip Length and Duration

Usually, we do not know the actual trip length and duration, except with the help of GPS/GIS. However, we can generally

TABLE V
FUEL CONSUMPTION COMPARISON

Drive cycle	Trip length (miles)	Trip duration (s)	Fuel consumption (Default algorithm) (kg)	Fuel consumption (Proposed algorithm) (kg)	Fuel savings (%)
4 LA92 cycles	39.24	5740	0.960	0.922	3.96
6 LA92 cycles	58.86	8610	1.959	1.883	3.88
2 REP05 cycles	40.08	2800	1.318	1.289	2.20
3 REP05 cycles	60.12	4200	2.473	2.404	2.79

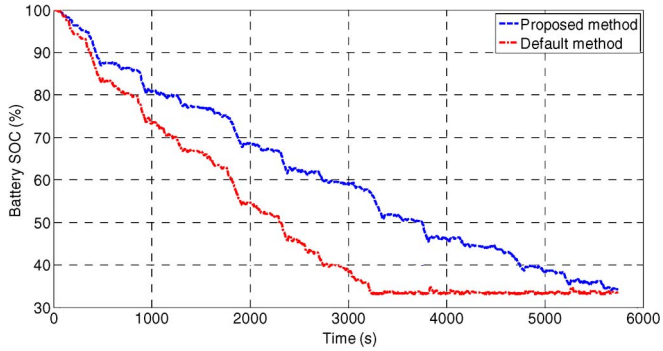

Fig. 19. Battery SOC comparison.

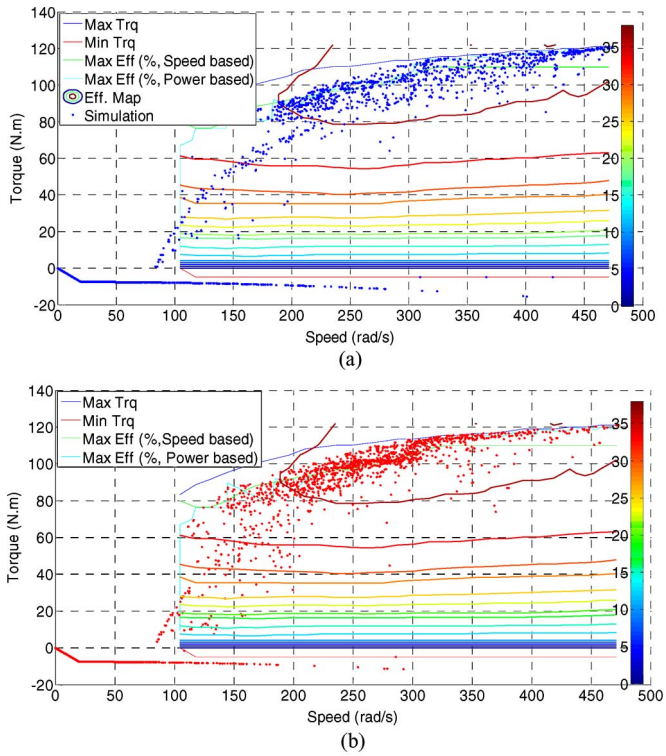

Fig. 20. Comparison of engine efficiency levels. (a) Default CS + CD algorithm. (b) Proposed controller.

estimate the trip distance by experience. The proposed algorithm is still feasible based on the estimated trip length and duration. To evaluate them, four consecutive Artemis drive cycles and seven New European drive cycles (NEDC) are simulated to validate the algorithm. With the default algorithm, the simulation result is shown in Table VI. The beginning SOC is 100%, and the total fuel consumption is 0.722 and 0.882 kg with the ending SOC of 31.36% and 31.53%, respectively.

TABLE VI
FUEL CONSUMPTION COMPARISON AND SOC COMPARISON

Drive cycle	Length (miles)	Duration (s)	Fuel consumption (kg)	Ending SOC (%)
4 Artemis cycles	40.86	3924	0.722	31.36
7 NEDC cycles	47.88	8267	0.882	31.53

To validate the performance of the proposed algorithm, we considered four groups of parameters for trip length and duration for each drive cycle, which are shown in Table VII. Groups 1–4 parameters are for four Artemis cycles and Groups 5–8 parameters are for seven NEDC cycles. Group 1 parameters are the actual trip parameters, and Groups 2 and 3 parameters are smaller and larger than the actual parameters. In Group 4, the trip length is larger, and the trip duration is shorter than the actual values. These three groups of parameters can reflect the differences of the estimated parameters. After simulation, the battery SOC curves based on different parameters are shown in Fig. 21. They are almost the same, and the ending SOC is 36.86%, 34.70%, 38.32%, and 34.03%, respectively. From Table VII, with the SOC correction included, we can see that the proposed controller can save 4.02%, 5.12%, 5.82%, and 3.74% of fuel consumption, compared with the default control algorithm. Table VII also compares the results for different trip lengths and duration when seven consecutive NEDC drive cycles are simulated. The ending SOC is 31.43%, 33.42%, 31.54%, and 34.62%, respectively, and the proposed controller can save 2.49%, 2.15%, 3.17%, and 3.51% of fuel consumption, respectively. Therefore, the results show that the controller can improve the fuel economy based on the estimated trip length and duration.

C. Simulation With Unknown Trip Length and Duration

Suppose that we do not know any information about the trip length and duration. Based on the proposed controller, the vehicle uses all the stored electric energy first until the SOC drops to 30%, and then N2 starts to work to output the battery current command to manage the power distribution. To validate the performance, three consecutive REP05 and four consecutive Artemis drive cycles are simulated.

The SOC variations based on the proposed controller and the default strategy are shown in Fig. 22 when three REP05 drive cycles are simulated. With the proposed controller, we can see that the SOC first drops to 30%, which is the same as that when applying the default algorithm. Then, the SOC maintains near 30%. Based on the training of the optimal results obtained by the DP method, N2 stores the optimal power distribution algorithm for different types of drive cycles, which makes the

TABLE VII
FUEL CONSUMPTION COMPARISON AND SOC COMPARISON

Drive cycle	Groups	Estimated trip length (miles)	Estimated trip duration (s)	Fuel consumption (SOC corrected) (kg)	Ending SOC (%)	Fuel savings (%)
4 Artemis cycles	Group 1	40.86	3924	0.693	36.86	4.02
	Group 2	40.00	3600	0.685	34.70	5.12
	Group 3	42.00	4200	0.680	38.32	5.82
	Group 4	42.00	3600	0.695	34.03	3.74
7 NEDC cycles	Group 5	47.88	8267	0.860	31.43	2.49
	Group 6	50.00	8500	0.863	33.42	2.15
	Group 7	45.00	8000	0.854	31.54	3.17
	Group 8	45.00	8500	0.851	34.62	3.51

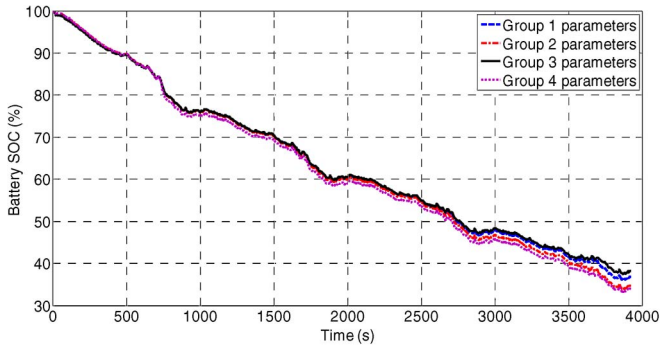

Fig. 21. SOC with different input parameters.

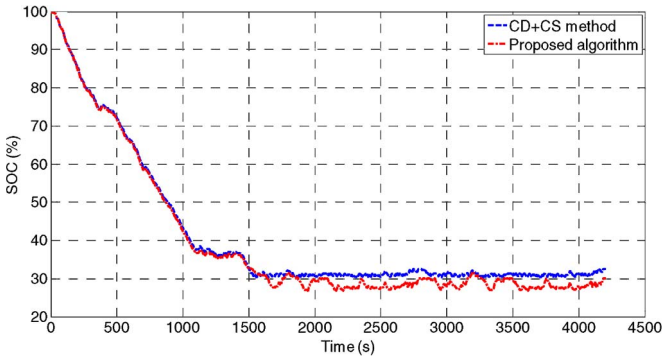

Fig. 22. SOC comparison.

TABLE VIII
FUEL CONSUMPTION COMPARISON

Drive cycle	Length (miles)	Fuel consumption (Default algorithm) (kg)	Fuel consumption (Proposed algorithm) (kg)	Fuel savings (%)
3 REP05 cycles	60.12	2.433	2.390	1.77
4 Artemis cycles	40.86	0.722	0.697	3.46

battery charge or discharge more frequently to ensure the engine works more efficiently. Fig. 22 shows that the SOC varies more obviously when the proposed controller is applied than that when the default controller is applied. The ending SOC based on the two algorithms is 32.5% and 30.08%. Table VIII lists the fuel consumption based on different algorithms. The proposed algorithm can save 1.77% and 3.46% of fuel consumption with SOC correction included when three REP05 and four Artemis drive cycles are simulated. When the total driving distance and the total driving duration are unknown, the proposed algorithm can still save fuel consumption compared with the default algorithm. However, the saving is less than that when the trip distance and duration is known, as presented in Tables V and VII.

VII. CONCLUSION

An effective online intelligent energy controller consisting of two NN control modules has been built to improve the fuel economy of a power-split PHEV. Based on whether the trip length and trip duration is known or unknown, the controller works differently to manage the energy distribution between the engine and the battery more intelligently, compared with the conventional CD and CS algorithm.

When the trip length and trip duration are known or can be estimated in advance and the trip length is more than the calculated AER, the controller will use N1 to calculate and generate the suboptimal battery current commands to manage the power distribution between the ICE and the battery in real time based on vehicle speed and other related parameters. If the trip length is less than the calculated AER, the vehicle will first use the battery to drive the vehicle. The simulation results validate the effectiveness of the controller.

If the controller cannot obtain the trip length and trip duration before the trip starts, the vehicle will be powered by the battery first until the battery SOC drops to a preset low threshold, and then the controller uses N2 to output the battery current commands. It can still improve the fuel economy.

In this paper, the controller has been only validated by simulation. Moreover, the controller does not consider the slope of the road, which can influence the vehicle driveline power. We also did not consider the battery aging and degradation issues, which can affect the AER as well as vehicle energy management. Our next research work will be carried out to consider improving the performance of the controller and validate the controller by experiment.

REFERENCES

[1] M. Ehsani, Y. Gao, and A. Emadi, *Modern Electric, Hybrid Electric, and Fuel Cell Vehicles: Fundamentals, Theory, and Design,* 2nd ed. New York, NY, USA: Taylor & Francis, 2009.

[2] V. Freyermuth, E. Fallas, A. Rousseau, and S. O. A. Engineers, "Comparison of Powertrain Configuration for Plug-in HEVs from a Fuel Economy Perspective," SAE Int., Warrendale, PA, USA, Tech. Rep. 2008-01-0461, 2008.

[3] L. Guzzella and A. Sciarretta, *Vehicle Propulsion Systems: Introduction to Modeling and Optimization*. New York, NY, USA: Springer-Verlag, 2010.
[4] C. Mi, A. Masrur, and D. W. Gao, *Hybrid Electric Vehicles: Principles and Applications with Practical Perspectives*. Hoboken, NJ, USA: Wiley, 2011.
[5] X. Zhang, *Power Systems: Vehicle Power Management: Modeling, Control and Optimization*. London, U.K.: Springer-Verlag, 2011.
[6] C. C. Chan, A. Bouscayrol, and K. Chen, "Electric, hybrid, and fuel-cell vehicles: Architectures and modeling," *IEEE Trans. Veh. Technol.*, vol. 59, no. 2, pp. 589–598, Feb. 2010.
[7] P. B. Sharer, A. Rousseau, D. Karbowski, and S. Pagerit, "Plug-in Hybrid Electric Vehicle Control Strategy: Comparison between EV and Charge-Depleting Options," SAE Int., Warrendale, PA, USA, SAE Tech. Paper 2008-01-0460, 2008.
[8] C. Zheng, F. Yuhong, and C. C. Mi, "State of charge estimation of lithium-ion batteries in electric drive vehicles using extended Kalman filtering," *IEEE Trans. Veh. Technol.*, vol. 62, no. 3, pp. 1020–1030, Mar. 2013.
[9] Z. Bingzhan, C. C. Mi, and Z. Mengyang, "Charge-depleting control strategies and fuel optimization of blended-mode plug-in hybrid electric vehicles," *IEEE Trans. Veh. Technol.*, vol. 60, no. 4, pp. 1516–1525, May 2011.
[10] Z. Chen, C. C. Mi, R. Xiong, J. Xu, and C. You, "Energy management of a power-split plug-in hybrid electric vehicle based on genetic algorithm and quadratic programming," *J. Power Sources*, vol. 248, pp. 416–426, Feb. 2014.
[11] Y. L. Murphey, P. Jungme, L. Kiliaris, M. L. Kuang, M. A. Masrur, A. M. Phillips, and W. Qing, "Intelligent hybrid vehicle power control—Part II: Online intelligent energy management," *IEEE Trans. Veh. Technol.*, vol. 62, no. 1, pp. 69–79, Jan. 2013.
[12] Y. L. Murphey, P. Jungme, C. Zhihang, M. L. Kuang, M. A. Masrur, and A. M. Phillips, "Intelligent hybrid vehicle power control—Part I: Machine learning of optimal vehicle power," *IEEE Trans. Veh. Technol.*, vol. 61, no. 8, pp. 3519–3530, Oct. 2012.
[13] C. Zheng and C. C. Mi, "An adaptive online energy management controller for power-split HEV based on dynamic programming and fuzzy logic," in *Proc. IEEE VPPC*, 2009, pp. 335–339.
[14] C. Zheng, Z. Xi, and C. C. Mi, "Slide mode and fuzzy logic based powertrain controller for the energy management and battery lifetime extension of series hybrid electric vehicles," *J. Asian Elect. Veh.*, vol. 8, no. 2, pp. 1425–1432, Dec. 2010.
[15] Z. Zhiguang, C. Mi, C. Zheng, A. Masrur, and Y. L. Murphey, "Power management of passive multi-source hybrid electric vehicle," in *Proc. IEEE VPPC*, 2011, pp. 1–4.
[16] K. Namwook, C. Sukwon, and P. Huei, "Optimal control of hybrid electric vehicles based on pontryagin's minimum principle," *IEEE Trans. Control Syst. Technol.*, vol. 19, no. 5, pp. 1279–1287, Sep. 2011.
[17] X. Li, J. Li, L. Xu, M. Ouyang, X. Han, L. Lu, and C. Lin, "Online management of lithium-ion battery based on time-triggered controller area network for fuel-cell hybrid vehicle applications," *J. Power Sources*, vol. 195, no. 10, pp. 3338–3343, May 2010.
[18] H. Xi, T. Ying, and H. Xingui, "An intelligent multifeature statistical approach for the discrimination of driving conditions of a hybrid electric vehicle," *IEEE Trans. Intell. Transp. Syst.*, vol. 12, no. 2, pp. 453–465, Jun. 2011.
[19] S. Stockar, V. Marano, M. Canova, G. Rizzoni, and L. Guzzella, "Energy-optimal control of plug-in hybrid electric vehicles for real-world driving cycles," *IEEE Trans. Veh. Technol.*, vol. 60, no. 7, pp. 2949–2962, Sep. 2011.
[20] M. Koot, J. T. B. A. Kessels, B. de Jager, W. P. M. H. Heemels, P. P. J. van den Bosch, and M. Steinbuch, "Energy management strategies for vehicular electric power systems," *IEEE Trans. Veh. Technol.*, vol. 54, no. 3, pp. 771–782, May 2005.
[21] J. T. B. A. Kessels, M. W. T. Koot, P. P. J. van den Bosch, and D. B. Kok, "Online energy management for hybrid electric vehicles," *IEEE Trans. Veh. Technol.*, vol. 57, no. 6, pp. 3428–3440, Nov. 2008.
[22] P. Jungme, C. Zhihang, L. Kiliaris, M. L. Kuang, M. A. Masrur, A. M. Phillips, and Y. L. Murphey, "Intelligent vehicle power control based on machine learning of optimal control parameters and prediction of road type and traffic congestion," *IEEE Trans. Veh. Technol.*, vol. 58, no. 9, pp. 4741–4756, Nov. 2009.
[23] S. Ebbesen, P. Elbert, and L. Guzzella, "Battery state-of-health perceptive energy management for hybrid electric vehicles," *IEEE Trans. Veh. Technol.*, vol. 61, no. 7, pp. 2893–2900, Sep. 2012.
[24] S. G. Li, S. M. Sharkh, F. C. Walsh, and C. N. Zhang, "Energy and battery management of a plug-in series hybrid electric vehicle using fuzzy logic," *IEEE Trans. Veh. Technol.*, vol. 60, no. 8, pp. 3571–3585, Oct. 2011.
[25] H. Borhan, A. Vahidi, A. M. Phillips, M. L. Kuang, I. V. Kolmanovsky, and S. Di Cairano, "MPC-based energy management of a power-split hybrid electric vehicle," *IEEE Trans. Control Syst. Technol.*, vol. 20, no. 3, pp. 593–603, May 2012.
[26] W. Lei, E. G. Collins, Jr., and L. Hui, "Optimal design and real-time control for energy management in electric vehicles," *IEEE Trans. Veh. Technol.*, vol. 60, no. 4, pp. 1419–1429, May 2011.
[27] P. Pisu and G. Rizzoni, "A comparative study of supervisory control strategies for hybrid electric vehicles," *IEEE Trans. Control Syst. Technol.*, vol. 15, no. 3, pp. 506–518, May 2007.
[28] Z. Zhou and C. Mi, "Power management of PHEV using quadratic programming," *Int. J. Elect. Hybrid Veh.*, vol. 3, no. 3, pp. 246–258, 2011.
[29] G. Qiuming, L. Yaoyu, and P. Zhong-Ren, "Trip based optimal power management of plug-in hybrid electric vehicles using gas-kinetic traffic flow model," in *Amer. Control Conf.*, 2008, pp. 3225–3230.
[30] G. Qiuming, L. Yaoyu, and P. Zhong-Ren, "Trip-based optimal power management of plug-in hybrid electric vehicles," *IEEE Trans. Veh. Technol.*, vol. 57, no. 6, pp. 3393–3401, Nov. 2008.
[31] Z. Menyang, Y. Yan, and C. C. Mi, "Analytical approach for the power management of blended-mode plug-in hybrid electric vehicles," *IEEE Trans. Veh. Technol.*, vol. 61, no. 4, pp. 1554–1566, May 2012.
[32] S. J. Moura, H. K. Fathy, D. S. Callaway, and J. L. Stein, "A stochastic optimal control approach for power management in plug-in hybrid electric vehicles," *IEEE Trans. Control Syst. Technol.*, vol. 19, no. 3, pp. 545–555, May 2011.
[33] R. E. Bellman, *Dynamic Programming*. Princeton, NJ, USA: Princeton Univ. Press, 1957.
[34] S. C. Fang and S. Puthenpura, *Linear Optimization and Extensions: Theory and Algorithms*. Englewood Cliffs, NJ, USA: Prentice-Hall, 1993.

Zheng Chen (A'10–M'12) received the B.S. and M.S. degrees in electrical engineering and the Ph.D. degree in control science engineering from Northwestern Polytechnical University, Xi'an, China, in 2004, 2007, and 2012, respectively.

From 2008 to 2011, he was a Visiting Scholar with the University of Michigan, Dearborn, MI, USA. He is currently a Postdoctoral Researcher with the Department of Electrical and Computer Engineering, University of Michigan–Dearborn. His research interests include battery management systems, battery status estimation, and energy management of hybrid electric vehicles.

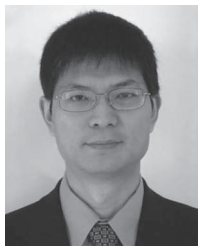

Chunting Chris Mi (S'00–A'01–M'01–SM'03–F'12) received the B.S. and M.S. degrees from Northwestern Polytechnical University, Xi'an, China, and the Ph.D. degree from the University of Toronto, Toronto, ON, Canada, all in electrical engineering.

Previously, he was an Electrical Engineer with General Electric Canada, Inc. He is currently a Professor of electrical and computer engineering and the Director of the newly established Department of Energy GATE Center for Electric Drive Transportation, University of Michigan, Dearborn, MI, USA. He has conducted extensive research and published more than 100 articles. His research interests include electric drives, power electronics, electric machines, renewable energy systems, and electrical and hybrid vehicles.

Dr. Mi was the Vice Chair of the IEEE Southeastern Michigan Section from 2006 to 2007, the Chair of the IEEE Southeastern Michigan Section from 2008 to 2009, and the General Chair of the Fifth IEEE Vehicle Power and Propulsion Conference held in Dearborn on September 6–11, 2009. He has served as a Guest Editor for the *International Journal of Power Electronics* and as an Associate Editor for the *Journal of Circuits, Systems, and Computers* from 2007 to 2009. He serves on the Editorial Board of the *International Journal of Electric and Hybrid Vehicles* and the *Institution of Engineering and Technology Electrical Systems in Transportation*. He has served as an Associate Editor for the IEEE TRANSACTIONS ON VEHICULAR TECHNOLOGY, the IEEE TRANSACTIONS ON POWER ELECTRONICS LETTERS, and the IEEE TRANSACTIONS ON INDUSTRY APPLICATIONS, and as a Senior Editor for the *IEEE Vehicular Technology Magazine*. He received the Distinguished Teaching Award and Distinguished Research Award from the University of Michigan–Dearborn, the 2007 IEEE Region 4 Outstanding Engineer Award, the IEEE Southeastern Michigan Section Outstanding Professional Award, and the SAE Environmental Excellence in Transportation Award.

Jun Xu (S'13) received the B.S. degree in mechanical engineering from Xi'an Jiaotong University, Xi'an, Shaanxi, China, in 2009. He is currently working toward the Joint Ph.D. degree in mechanical engineering with the School of Mechanical Engineering, Xi'an Jiaotong University, and with the Department of Electrical and Computer Engineering, University of Michigan, Dearborn, MI, USA, where he focused on battery management systems for electric vehicles, hybrid electric vehicles, and applications of plug-in hybrid electric vehicles.

His research interests include design, analysis, testing, and state estimation of battery systems, particularly battery modeling, battery state estimation, and battery balancing.

Xianzhi Gong received the B.S. degree in electrical engineering and automation from Nanjing University of Aeronautics and Astronautics, Nanjing, China, in 2009 and the M.S. degree from the University of New Haven, West Haven, CT, USA, in 2011. He is currently working toward the Ph.D. degree in automotive systems engineering from the Department of Electrical and Computer Engineering, University of Michigan, Dearborn, MI, USA.

His current research interests include battery management, renewable energy, and power electronics.

Chenwen You received the B.S. degree in electrical engineering and automation from Huazhong University of Science and Technology, Wuhan, China, in 2010 and the M.S. degree in electrical engineering from the University of Michigan, Dearborn, MI, USA. She is currently working toward the Ph.D. degree in automotive systems engineering with the Department of Electrical and Computer Engineering, University of Michigan–Dearborn.

Her current research interests include power electronics, wireless chargers, and power management in hybrid electric vehicles.